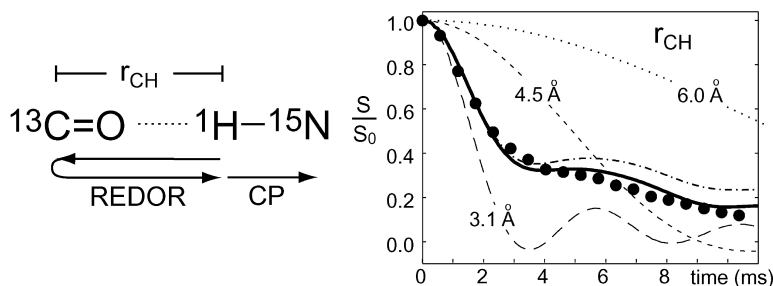


Measurements of Carbon to Amide-Proton Distances by C–H Dipolar Recoupling with N NMR Detection

Klaus Schmidt-Rohr, and Mei Hong

J. Am. Chem. Soc., **2003**, 125 (19), 5648-5649 • DOI: 10.1021/ja0344415 • Publication Date (Web): 22 April 2003

Downloaded from <http://pubs.acs.org> on March 26, 2009



More About This Article

Additional resources and features associated with this article are available within the HTML version:

- Supporting Information
- Links to the 6 articles that cite this article, as of the time of this article download
- Access to high resolution figures
- Links to articles and content related to this article
- Copyright permission to reproduce figures and/or text from this article

[View the Full Text HTML](#)



ACS Publications
 High quality. High impact.

Measurements of Carbon to Amide-Proton Distances by C–H Dipolar Recoupling with ^{15}N NMR Detection

Klaus Schmidt-Rohr and Mei Hong*

Department of Chemistry, Iowa State University, Ames, Iowa 50011

Received January 31, 2003; E-mail: mhong@iastate.edu

Internuclear distance measurements are an important aspect of solid-state nuclear magnetic resonance (NMR) structure determination of biomolecules. The most frequently used method for determining heteronuclear distances is rotational-echo double resonance (REDOR), where rotor-synchronized 180° pulses recouple the heteronuclear dipolar interaction under magic-angle spinning (MAS).^{1–5} In proteins, ^{13}C – ^{15}N internuclear distances are usually measured using specifically ^{13}C , ^{15}N -labeled samples.^{6,7} However, the relatively small magnetic dipole moment of ^{15}N limits the maximum distance detectable.

In this Communication, we demonstrate how additional important internuclear distances, between the ^{13}C and the amide proton (H^{N}) bonded to the amide ^{15}N , can be determined up to at least 6 Å. The ^{13}C – H^{N} distance is particularly important for defining the hydrogen bonding geometry between $^{13}\text{C}=\text{O}$ and $\text{H}^{\text{N}}\text{--}^{15}\text{N}$ groups. Because of the 10-fold difference between the ^1H and ^{15}N magnetic dipole moments and the multiple-pulse scaling factor of about 0.5, the effective ^{13}C – ^1H dipolar interaction in our technique is 5-fold stronger than the ^{13}C – ^{15}N dipolar coupling for the same internuclear distance. In addition, in hydrogen bonded $^{13}\text{C}=\text{O}\cdots\text{H}^{\text{N}}\text{--}^{15}\text{N}$ systems, the relevant internuclear ^{13}C – $^1\text{H}^{\text{N}}$ distance is typically reduced by ~ 1 Å as compared to the ^{13}C – ^{15}N distance.^{8,9} Thus, the effective ^{13}C – $^1\text{H}^{\text{N}}$ coupling will be about 10 times stronger than the corresponding ^{13}C – ^{15}N interaction. This large coupling strength permits distances up to at least 6 Å to be determined reliably.

Figure 1 shows the pulse sequence for this ^{15}N -detected C–H REDOR experiment. As in the related medium- and long-distance (MELODI) heteronuclear correlation technique,^{10,11} the magnetization of each proton initially evolves in the dipolar field of the ^{13}C spin. The ^1H homonuclear couplings are suppressed by a multiple-pulse decoupling sequence. As indicated in Figure 1a, we used MREV-8¹² without special tune-up and found it to be highly effective for amide protons bonded to ^{15}N nuclei, yielding ^1H T_2 relaxation times of up to 5 ms. Because undisturbed MAS averages out the C–H dipolar interaction, two ^{13}C 180° pulses per rotation period are applied to recouple the C–H dipolar interaction, as is common in REDOR experiments. The ^1H isotropic chemical shift is refocused by a ^1H 180° pulse in the center of this C–H dephasing period. The magnetization of each proton is modulated independently by its coupling to the ^{13}C nucleus, resulting in simple spin-pair REDOR curves that depend only on the C–H internuclear distance. To selectively detect the modulation of the H^{N} magnetization, a short Lee–Goldburg cross polarization^{13–15} from ^1H to ^{15}N is applied before ^{15}N detection. The dephased signal S is recorded as a function of the C–H dephasing time t_{CH} . The reference signal S_0 , without the C–H dipolar dephasing but otherwise with identical relaxation behavior, is obtained by switching off the ^{13}C 180° recoupling pulses. The normalized dephasing S/S_0 , plotted as a function of t_{CH} , depends exclusively on the C– H^{N} distance.

When the ^{13}C – $^1\text{H}^{\text{N}}$ distance of interest is large, dephasing of the H^{N} proton by nearby natural-abundance ^{13}C (1.1%) produces

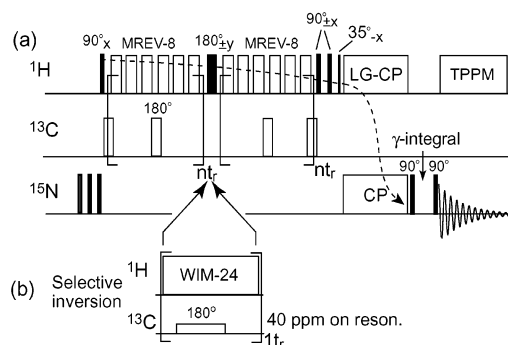


Figure 1. Pulse sequence for ^{15}N -detected ^{13}C – ^1H REDOR NMR. (a) Basic sequence. ^1H magnetization evolves under the influence of the recoupled ^{13}C – ^1H dipolar coupling, while homonuclear couplings are removed by multiple-pulse irradiation. We used six cycles of MREV-8 per rotor period, $3.4 \mu\text{s}$ 90° ^1H pulses, and a cycle time of $48 \mu\text{s}$. Each ^{13}C 180° pulse is simultaneous with a long window of MREV-8 and the following ^1H pulse. A short (50 – $100 \mu\text{s}$) Lee–Goldburg CP from ^1H to ^{15}N and a z-filter incremented in two steps of $\tau_z/2$ (γ -integral¹⁶) were applied before ^{15}N detection. (b) Selective inversion scheme to reduce dephasing by natural-abundance ^{13}C sites. ^1H evolution during the soft ^{13}C pulse is minimized by the WIM-24 time-suspension sequence. In $^{13}\text{C}\alpha$, ^{15}N -labeled *N*-*t*-BOC-glycine, the inversion pulse reduced aliphatic-carbon-induced dephasing of H^{N} protons by a factor of 5.

detectable dephasing. For instance, a reduction of $\Delta S/S_0$ by 15% is expected and observed (not shown) after 6 ms of MREV-8 decoupling in a typical ^{15}N -labeled peptide. For measurements of ^{13}CO – H^{N} distances, this effect can be minimized by adding a selective-pulse scheme,⁷ as indicated in Figure 1b. The natural-abundance aliphatic-carbon coherence can be inverted by a soft on-resonance 180° pulse and thus does not dephase the protons, while the $^{13}\text{C}=\text{O}$ signal remains essentially unaffected. We applied a $73 \mu\text{s}$ 180° pulse, corresponding to a field strength of 6.8 kHz, at the 40 ppm ^{13}C frequency. This inverts the aliphatic carbons over a total range of ca. ± 30 ppm. The ^{13}CO coherence nutates around an effective field that makes an angle of 27° with the z -axis. Its isotropic-shift component undergoes a 390° rotation and thus returns mostly to the z -axis, without having had more than a minor transverse component that could be affected by CSA evolution. To prevent ^1H evolution during the ^{13}C pulse, a time-suspension sequence with vanishing average Hamiltonian, for example, WIM-24,¹⁷ is applied to the ^1H spins. The rotor synchronization of REDOR requires this time to be one rotation period, even if the ^{13}C pulse is shorter.

Figure 2 shows experimental ^{15}N -detected REDOR dephasing of the H^{N} magnetization by the $^{13}\text{C}\alpha$ spin in $^{13}\text{C}\alpha$, ^{15}N -labeled *N*-*t*-BOC-glycine. The data were collected without the selective inversion pulse (Figure 1a) because the coupling of interest is strong. The two-bond $\text{C}\alpha$ – H^{N} distance in this compound is 2.18 Å. The curve simulated using this distance and the ideal MREV-8 scaling factor of 0.47 agrees well with the experimental data (●). The

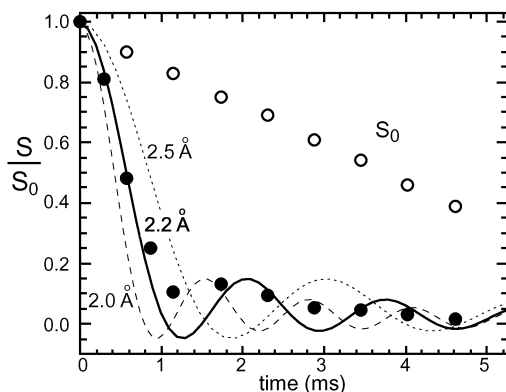


Figure 2. ^{13}C – H^{N} distance measurements in $^{13}\text{C}\alpha,^{15}\text{N}$ -labeled *N*-*t*-BOC-glycine by ^{15}N -detected ^{13}C – ^1H REDOR (with $50\ \mu\text{s}$ ^1H – ^{15}N CP). The normalized C–H dephasing (●) is recorded as a function of the C–H REDOR time using the sequence of Figure 1a. Also shown are calculated REDOR curves for three C–H distances, including the best-fit distance of 2.2 Å. The ○ symbols show the T_2 decay of the reference intensity S_0 , which should be as slow as possible to maximize the sensitivity of the experiment. The experiments were performed using a Bruker DSX-400 spectrometer and a triple-resonance probe at a spinning speed of 3.47 kHz for the 4 mm rotor. The ^1H multiple-pulse decoupling works best in this slow-spinning regime. For selectively labeled samples, faster spinning does not provide any significant enhancement in resolution or sensitivity.

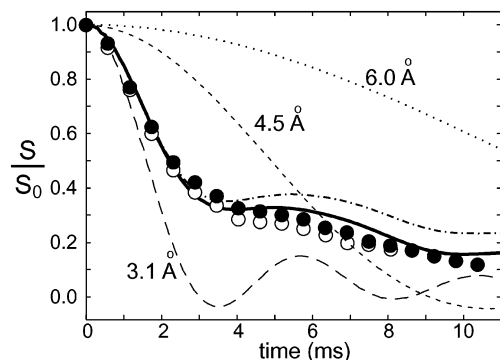


Figure 3. Intermolecular ^{13}CO – H^{N} distances in a 50:50 mixture of ^{13}CO -labeled and ^{15}N -labeled *N*-*t*-BOC-glycine measured by ^{15}N -detected ^{13}C – ^1H REDOR (with $100\ \mu\text{s}$ ^1H – ^{15}N CP). ○ (to 8 ms): S/S_0 obtained using the pulse sequence of Figure 1a. ●: S/S_0 obtained including the selective inversion of Figure 1b. The undesirable dephasing by natural-abundance aliphatic ^{13}C sites has been reduced. Thick line: parameter-free fit based on the crystal structure of *N*-*t*-BOC-glycine and statistical labeling. For simplicity, the minor effects of two-carbon dephasing of H^{N} were treated using a spin-pair approximation. Other curves indicate the REDOR curves for single C–H distances of 3.1 Å (---), 4.5 Å (- - -), and 6.0 Å (· · ·). The dash-dotted curve indicates how a simulation omitting a 4.5 Å intermolecular distance that occurs with only 12.5% probability would lead to a clear discrepancy with the experimental data.

reference intensity S_0 (○) decreases with a relatively long T_2 time of 5 ms, indicating efficient homonuclear decoupling of the amide proton.

The ability of this method to reliably detect much longer, intermolecular ^{13}CO – H^{N} distances is demonstrated in Figure 3. In a 50:50 mixture of ^{13}COO -labeled and ^{15}N -labeled *N*-*t*-BOC-glycine, the contacts between the ^{13}COO and H^{N} – ^{15}N moieties are all intermolecular. Figure 3 shows the ^{15}N -detected C–H REDOR

data acquired without (○) and with (●) the desirable selective inversion of natural-abundance aliphatic ^{13}C . The thick line is the calculated dephasing curve based on the crystal structure and the 50% ^{13}COO labeling. This simulation fits the experimental data quite well without any adjustable parameters. The crystal structure shows the closest ^{13}COO and H^{N} contacts of 2.85 and 3.25 Å for the two molecules in the asymmetric unit cell.¹⁸ These are indicative of hydrogen bonding. The fast initial decay results from these nearest-neighbor distances and exhibits the characteristic oscillation found in a simulation for a 3.1 Å distance (---). Because of the statistical labeling, 50% of all ^{15}N have the nearest ^{13}COO neighbors at longer distances, causing slower decay at longer times. If a 4.5 Å intermolecular distance that occurs with only 12.5% probability is omitted from the simulation (dash-dotted line), then a clear discrepancy with the experimental data is observed. This indicates that long C–H distances are accurately detected by this technique. Finally, the calculated C–H REDOR curves for 4.5 Å (- - -) and 6.0 Å (· · ·) show that significant dephasing can be readily detected even for these long distances.

The ^{15}N -detected C–H REDOR experiment introduced here should be applied routinely whenever ^{13}C – ^{15}N REDOR is used to characterize a biomolecular structure. It promises to provide particularly useful information on CO– H^{N} hydrogen bonding. The new approach can be further developed in many ways, such as incorporating ^1H or ^{13}C chemical shift evolution, or using ^{15}N -induced dephasing and ^{13}C detection in uniformly labeled peptides and proteins.

Acknowledgment. M.H. thanks the Petroleum Research Fund and the National Science Foundation (MCB-0093398) for support of this research. K.S.-R. and M.H. both acknowledge the Sloan Foundation for Research Fellowships.

References

- Gullion, T.; Schaefer, J. J. *Magn. Reson.* **1989**, *81*, 196–200.
- Gullion, T.; Pennington, C. H. *Chem. Phys. Lett.* **1998**, *290*, 88–93.
- Liiyak, O.; Zax, D. B. *J. Chem. Phys.* **2000**, *113*, 1088–1096.
- Mueller, K. T.; Jarvie, T. P.; Aurentz, D. J.; Roberts, B. W. *Chem. Phys. Lett.* **1995**, *242*, 535–542.
- Jaroniec, C. P.; Filip, C.; Griffin, R. G. *J. Am. Chem. Soc.* **2002**, *124*, 10728–10742.
- Hing, A. W.; Tjandra, N.; Cottam, P. F.; Schaefer, J.; Ho, C. *Biochemistry* **1994**, *33*, 8651–8661.
- Jaroniec, C. P.; Tounge, B. A.; Herzfeld, J.; Griffin, R. G. *J. Am. Chem. Soc.* **2001**, *123*, 3507–3519.
- Gu, Z.; Ridenour, C. F.; Bronnimann, C. E.; Iwashita, T.; McDermott, A. *J. Am. Chem. Soc.* **1996**, *118*, 822–829.
- Wei, Y.; Lee, D.; Ramamoorthy, A. *J. Am. Chem. Soc.* **2001**, *123*, 6118–6126.
- Yao, X. L.; Schmidt-Rohr, K.; Hong, M. *J. Magn. Reson.* **2001**, *149*, 139–143.
- Yao, X. L.; Hong, M. *J. Biomol. NMR* **2001**, 263–274.
- Rhim, W.-K.; Elleman, D. D.; Vaughan, R. W. *J. Chem. Phys.* **1973**, *59*, 3740–3749.
- Lee, M.; Goldberg, W. I. *Phys. Rev.* **1965**, *140*, A1261–A1271.
- vanRossum, B. J.; deGroot, C. P.; Ladizhansky, V.; Vega, S.; deGroot, H. J. M. *J. Am. Chem. Soc.* **2000**, *122*, 3465–3472.
- Ladizhansky, V.; Vega, S. *J. Chem. Phys.* **2000**, *112*, 7158–7168.
- deAzevedo, E. R.; Bonagamba, T. J.; Hu, W.; Schmidt-Rohr, K. *J. Chem. Phys.* **2000**, *112*, 8988–9001.
- Caravatti, P.; Braunschweiler, L.; Ernst, R. R. *Chem. Phys. Lett.* **1983**, *100*, 305–310.
- Semertzidis, M.; Matsoukas, J.; Nastopoulos, V.; Hondrelis, J.; Voliotis, S. *Acta Crystallogr.* **1989**, *C45*, 1474–1475.

JA0344415